


SHORT COMMUNICATION

Downregulation of the schizophrenia risk-gene *Dgcr2* alters early microcircuit development in the mouse medial prefrontal cortex

Aude Molinard-Chenu^{1,2}  | Michel Godel^{1,2} | Alicia Rey^{1,2} | Stefano Musardo² |
Timea Bodogan² | Laszlo Vutskits^{2,3} | Camilla Bellone² | Alexandre Dayer^{1,2†}

¹Department of Psychiatry, University of Geneva Medical School, Geneva, Switzerland

²Department of Basic Neurosciences, University of Geneva Medical School, Geneva, Switzerland

³Department of Anesthesiology, Pharmacology, Intensive Care and Emergency Medicine, University Hospitals of Geneva, Geneva, Switzerland

Correspondence

Aude Molinard-Chenu, Department of Psychiatry, University of Geneva Medical School, Geneva 4 CH-1211, Switzerland.
Email: aude.molinard-chenu@hcuge.ch

Funding information

NCCR Synapsy, Grant/Award Number: 51NF40-185897; Vachoux Foundation; Institute of Genetics and Genomics of Geneva

Abstract

Alterations in the generation, migration and integration of different subtypes of neurons in the medial prefrontal cortex (mPFC) microcircuit could play an important role in vulnerability to schizophrenia. Using in vivo cell-type specific manipulation of pyramidal neurons (PNs) progenitors, we aim to investigate the role of the schizophrenia risk-gene DiGeorge Critical Region 2 (*Dgcr2*) on cortical circuit formation in the mPFC of developing mice. This report describes how *Dgcr2* knock down in upper-layer PNs impacts the functional maturation of PNs and interneurons (INs) in the mPFC. First, we demonstrate that *Dgcr2* knock-down disrupts laminar positioning, dendritic morphology and excitatory activity of upper-layer PNs. Interestingly, inhibitory activity is also modified in *Dgcr2* knock-down PNs, suggesting a broader microcircuit alteration involving interneurons. Further analyses show that the histological maturation of parvalbumin (PV) INs is not dramatically impaired, thus implying that other INs subtypes might be at play in the reported microcircuit alteration. Overall, this study unravels how local functional

List of Abbreviations: aCSF, artificial cerebrospinal fluid; C.I., confidence interval; cDNA, circular deoxyribonucleic acid; CTIP2, COUP-TF-interacting protein 2; DAPI, 4',6-diamidino-2-Phenylindole; *Dgcr2*, DiGeorge Critical Region 2; E14.5, embryonic day 14.5; GAD67, glutamic acid decarboxylase 1; GFP, green fluorescent protein; i.p., intraperitoneal; IHC, immunohistochemistry; INs, interneurons; L2/3, layer 2-3; mEPSC, miniature excitatory post-synaptic currents; mPFC, medial prefrontal cortex; NHS, normal horse serum; O.N., overnight; PBS, phosphate buffer saline; PFA, paraformaldehyde; PNN, perineuronal nest; PNs, pyramidal neurons; PSC, post-synaptic currents; PV, parvalbumin; ROI, region of interest; RT, room temperature; S.D., standard deviation; Scram, scramble; sfGFP, superfolder green fluorescent protein; shRNA, short hairpin ribonucleic acid; sIPSC, spontaneous inhibitory post-synaptic currents; TOM, tomato; VZ, ventricular zone; WFA, *Wisteria floribunda* agglutinin.

†Deceased.

This is an open access article under the terms of the Creative Commons Attribution-NonCommercial-NoDerivs License, which permits use and distribution in any medium, provided the original work is properly cited, the use is non-commercial and no modifications or adaptations are made.

© 2022 The Authors. *International Journal of Developmental Neuroscience* published by John Wiley & Sons Ltd on behalf of International Society for Developmental Neuroscience.

deficits of the early postnatal development of the mPFC can be induced by *Dgcr2* knock-down in PNs.

KEYWORDS

corticogenesis, DGCR2, mPFC, projection neuron, schizophrenia

1 | INTRODUCTION

Schizophrenia is a complex neurodevelopmental disorder involving genetic vulnerabilities that affect the formation of cortical circuits including the medial prefrontal cortex (mPFC) as a key region in the modulation of dysfunctional behaviors associated to schizophrenia (Schubert et al., 2015). Cortical microcircuits integrity relies on the precise construction of their network architecture, including the positioning of neurons within cortical layers and their associated synaptic connectivity and plasticity. These processes are disrupted in rodent models of schizophrenia (Crabtree & Gogos, 2014), but the specific contribution of different neuronal populations is only starting to be unraveled (Glausier & Lewis, 2018). The migration of pyramidal neurons (PNs) (Muraki & Tanigaki, 2015) and the maturation and plasticity of their dendritic spines (Glausier & Lewis, 2013) participate in the cortical deficits observed in schizophrenia. Besides, interneurons (INs) are increasingly involved in pathophysiological processes of schizophrenia (Lewis, 2014; Lewis et al., 2005; Steullet et al., 2017). Among the various types of cortical INs, parvalbumin (PV) expressing INs appear as a critical subpopulation, maintaining a proper excitatory/inhibitory balance in the mPFC (Ferguson & Gao, 2018) by perisomatic inhibition of PNs (Freund & Katona, 2007). An important feature of PV INs maturation is the acquisition of perineuronal nests (PNN) (Berretta et al., 2015) containing extracellular matrix proteins such as *Wisteria floribunda* agglutininin (WFA). Functional dysmaturation patterns of PV INs in the mPFC have been described in schizophrenia animal models (Cabungcal et al., 2014) and post-mortem studies of schizophrenia patients (Curley et al., 2011; Enwright et al., 2016).

Dgcr2 is a schizophrenia-risk gene regulating the migration of cortical pyramidal neurons (PNs) in the primary sensory cortex (Molinard-Chenu & Dayer, 2018) but evidence is missing regarding the role it plays in the mPFC as well as in the functional maturation of cortical microcircuits. Here, we aim to describe how *Dgcr2* knock-down in upper-layer PNs impacts the post-natal maturation of the mPFC, assessing both morphological and electrophysiological properties of PNs and INs in the local microcircuit.

2 | MATERIALS AND METHODS

2.1 | In utero electroporation

Animal experiments were conducted according to the Swiss and International Guidelines, and approved by the local animal care committee (approval license number GE/78/14, GE113/116, GE/176/17). Embryos from time pregnant E14.5 CD1 mice (*Mus musculus*) were electroporated in the medial ventricular zone (VZ) of the dorsal pallium as described in (Niwa et al., 2010). For all analysis, pups were not selected based on sex and were randomly assigned to one or the other condition during in utero electroporation.

2.2 | Tissue processing and immunohistochemistry

Animals were euthanized by lethal i.p. injection of pentobarbital (50 mg/kg) at the mentioned developmental age and were then perfused with intracardial 0.9% saline followed by cold 4% PFA; 60- μ m-thick brain slices were cut at on a Vibratome (Leica VT100S) for immunohistochemistry (IHC). Sections were kept at 4°C in 0.1 M phosphate buffer saline (PBS) or at -20°C in a cryoprotective solution (37.5% ethylene glycol, 1.2% sucrose in phosphate buffer 0.05 M, pH = 7.4). Free-floating brain slices were incubated for 1h30 at room temperature (RT) in blocking solution (PBS, 2% normal horse serum [NHS], 0.5% Triton X-100) and incubated O.N. at 4°C in primary antibodies diluted in the blocking solution (rat anti-CTIP2, Abcam ab18465, 1:500, goat anti-GFP, Abcam ab5450, 1:2000, biotin-conjugated anti-WFA, Sigma, 1:2000, mouse anti-PV, Swant, 1:2000, goat anti-TOM, Sicgen, 1:300, mouse anti-GAD67, Merck-Millipore, 1:500). Slices were washed three times with PBS and incubated at RT for 1h30 in secondary antibodies diluted 1:500 in PBS, 2% NHS. Slices were washed three times with PBS and counterstained with Hoechst (diluted in PBS 1:10,000) for 10 min.

2.3 | Dendritic trees and spines analysis

Image stacks (1- μm stepped) of the basal dendrites of Lucifer-yellow injected PNs in the superficial layers of the mPFC were obtained with a Nikon A1r Spectral confocal microscope. The dendritic arbors were traced using Neurolucida software (Microbrightfield, USA) and total dendritic length, number of branching points and Scholl analysis were quantified.

Image stacks (0.41- μm stepped) of the second-order basal dendrites of Lucifer-yellow injected PNs in the superficial layers of the mPFC were obtained with a Zeiss LSM 700 confocal microscope. Dendritic spines density was analyzed using the cell counter plugin on Fiji software and their morphology was studied on OsiriX using the “spine counter” plug-in as in de Roo and Ribic (2017). The length of each spine was measured from the base to the tip of the protrusion. The width of the spines was determined as the largest diameter of the head amongst all image stacks. The spines were then morphologically classified using their length and width, determining their type (mushroom, stubby or thin) as in Haws et al. (2014). All dendritic analyses have been performed blind to experimental conditions.

2.4 | Electrophysiological recordings

Ex vivo electrophysiological recordings were performed using 200- to 250- μm -thick coronal mPFC slices prepared from P30 mice previously electroporated as described above. Brains were sliced in an artificial cerebrospinal fluid (aCSF), bubbled with 95% O_2 and 5% CO_2 and incubated for 20–30 min at 35°C. Subsequently, slices were transferred at room temperature or in the recording chamber at 34–37°C in aCSF. Whole-cell voltage clamp electrophysiological recordings were conducted at -70 mV. Post-synaptic currents (PSC) were recorded from mPFC L2/3 PNs in the presence of 3 mM kynurenic acid for spontaneous inhibitory post-synaptic currents (sIPSC) and picrotoxin (100 μM) and TTX (1 μM) for miniature excitatory post-synaptic currents (mEPSC). The patch pipettes were filled with (in mM) 130 CsCl, 1.0 MgCl_2 , 10.0 HEPES, 0.05 EGTA, 5.0 Mg-ATP , 5.0 QX-314, pH adjusted to 7.3 with CsOH, osmolarity to 288 mOsm. PSCs were collected with a Multiclamp 700B-amplifier (Axon Instruments, Foster City, CA), filtered at 2.2 kHz, digitized at 5 kHz and analyzed using MiniAnalysis 6 (Synaptosoft) software. Electrophysiology experiments were performed blind to experimental conditions.

2.5 | Statistical analysis

Statistical analyses on continuous variables were performed on Prism software (GraphPad Software, La Jolla California, USA), and normality of the samples was tested by Shapiro–Wilk test. Sample sizes and relevant statistical tests are specified for each result in the results section, on the figures or in the figures legends. We used IBM® SPSS® Statistics v26.0.0.0 for macOS (Armonk, NY: IBM Corp.) for analyses on categorical variables. To perform post hoc analyses on contingency tables, we applied the method described in Beasley and Schumacker (1995). For the analysis of the basal dendritic arbor complexity, we used a mixed model regression analysis as described in Mancini et al. (2020) and Mutlu et al. (2013).

2.6 | Plasmids and shRNAs

All constitutive expressions of shRNAs and cDNAs were driven by the human U6 promoter, in the PLKO.1 vector for the shRNAs and pUB6/V5-His A (pUB6) vector for the cDNAs. The following shRNAs were electroporated in equal ratios in control and experimental conditions: *Dgcr2* shRNA (TRCN0000094432 mature sense: CCCGTCCTTATGGGAAGGAAA, ThermoFisher) and *Scrambled* shRNA (mature sense: CCTAAGGTTAAGTCGCCCTCG, Addgene). Typically, shRNAs were injected at a concentration of 1 $\mu\text{g}/\mu\text{l}$ together with tdTomato or sfGFP at concentrations 0.5–2 $\mu\text{g}/\mu\text{l}$. The effectiveness of *Dgcr2* shRNA was described in Molinard-Chenu and Dayer (2018), it allows a significant reduction in the protein expression of *Dgcr2*, both in vivo and in vitro.

2.7 | Iontophoretic post hoc single cell injection

P30 mice, electroporated at E14.5, were sacrificed by pentobarbital (100 mg/kg) intraperitoneal injection (i.p.) and transcardially perfused first with 0.9% NaCl + heparin (10,000 units/L) solution, then with a mixture of 4% PFA and 0.125% glutaraldehyde (pH 7.4). After removal, brains were fixed in 4% PFA for 2 h, and then rinsed in 0.1 M phosphate-buffered saline (PBS, pH 7.4). The 300- μm -thick coronal sections were cut on a vibratome (Leica, Germany) in ice-cold PBS. Sections were stained in 1% methylene blue (Bichsel, Switzerland) for 10 min to visualize the cell bodies. Section were placed in a PBS-containing chamber under an epifluorescent microscope (Olympus, Japan) equipped with a micromanipulator.

Tomato expressing cells were loaded with 5% Lucifer Yellow (Sigma-Aldrich, USA) solution by a sharp glass capillary using negative current. All solutions and the brain tissues were kept at 4°C during the whole procedure. To detect Lucifer Yellow (LY), sections were pre-incubated in a PBS solution containing 5% sucrose, 2% bovine serum albumin (BSA), 1% Triton X-100 and 0.1% Na-azide for 1 h at room temperature. The same solution containing rabbit anti-LY primary antibody (Invitrogen, USA) in 1:4000 dilution was used for immunolabeling for 48 h at room temperature. After three-times 20 min washing in PBS, incubation with an Alexa Flour 488 conjugated anti-rabbit secondary antibody (Invitrogen, USA) diluted 1:1000 in the pre-incubation solution was performed for 24 h at room temperature. Three-times 20 min washing in PBS was followed by incubation of the slices in 1:5000 diluted Hoechst 33342 solution (Invitrogen, USA) for 20 min to stain cell nuclei. After two-times 20 min washing in PBS, sections were mounted, dried and covered with Immu-mount (Fischer Scientific, USA) and glass coverslips.

2.8 | Image acquisition, processing and data analysis

Images were obtained on an epifluorescence microscope (Nikon Eclipse 90i) for the laminar positioning study, a confocal microscope (Zeiss Axio Imager Z.2) for the PV INs study, and Figure 2a was obtained on a confocal microscope (Nikon A1R). All described image analyses were done using Fiji, using the following plugins: cell counter, analyze particles. For the laminar positioning analysis, regions of interest (ROI) for upper and lower layers were drawn including the average width of upper layers, based on IHC for CTIP2 (delimitating the layers 5–6) in two control brains. PV + INs were analyzed in the mPFC including all cortical layers, based on DAPI. For the PV INs intensity study, circle ROI including the soma of PV + INs was analyzed; the arbitrary unit corresponds to their mean integrated density normalized on the mean intensity of three ROIs in the background of the same image and cells were then classified as low, intermediate low, intermediate high or high intensity depending on their quartile in the distribution of the total PV cells intensity. For the perisomatic GAD67 analysis, ROI were created using a 15 px selection brush contouring manually each electroporated PN, and their mean integrated density was obtained as described previously. Image analysis were performed blind to the experimental condition, except for the laminar positioning study.

3 | RESULTS AND DISCUSSION

Using in utero electroporation targeted to PN progenitors in the mPFC at E14.5, we observed a higher percentage of PNs in layers 5–6 and in the white matter in *Dgcr2* knock-down condition compared with control condition at P0.5 (Figure S1), thus demonstrating the role of *Dgcr2* in the laminar positioning of PNs in the mPFC at P0.5. In order to assess the effect of *Dgcr2* knock-down on dendritogenesis, we performed a morphological analysis of the proximal basal dendrites of P30 layer 2/3 PNs previously electroporated at E14.5 with either *Dgcr2* or *Scramble* (*scram*) shRNA (Figure 1a). Scholl analysis, using a mixed model regression analysis, revealed an altered complexity of the dendritic arbor in *Dgcr2* knock-down PNs, especially in the proximal radii (Figure 1b,c). The overall density of the second order basal dendritic spines was not affected by *Dgcr2* knock-down (Figure 1d), but morphology analysis of these dendritic spines showed a disrupted maturation pattern in *Dgcr2* knock-down PNs (Figure 1e–g, Table S1). Indeed, the length and width of basal dendritic spines as well as the relative proportion of “mushroom” dendritic types were lower in *Dgcr2* knock-down PN. These results suggest that *Dgcr2* knock-down impacts the functional maturation of PNs in the mPFC, leading to potential consequences on their activity. In order to further test this hypothesis, we recorded miniature Excitatory Post-Synaptic Currents (mEPSC) and spontaneous Inhibitory Post-Synaptic Currents (sIPSC) in L2/3 PNs (previously electroporated at E14.5 with *Scram* or *Dgcr2* shRNA) in the mPFC at P30. In line with the deficits observed in dendritic maturation, we also observed a decrease in the frequency and in the amplitude of mEPSC in *Dgcr2* knock-down PNs (Figure 2a,b). Interestingly, the amplitude and the frequency of sIPSC were also decreased in *Dgcr2* knock-down PNs (Figure 2c,d), suggesting that downregulation of *Dgcr2* in PNs indirectly affects the activity of inhibitory interneurons (INs) in the mPFC microcircuit. Given the putative role of mPFC PV-expressing INs in the physiopathology of schizophrenia and their functional relevance in the mPFC microcircuit (Ferguson & Gao, 2018), we next assessed the maturation of PV INs in our model. At P30, in the mPFC ipsilateral to the electroporation site, the cellular density of PV INs was unchanged by *Dgcr2* knock-down, and the mean fluorescence intensity of PV INs as well as the distribution of low to high intensity PV INs was also not altered by *Dgcr2* knock-down (Figure 3a–d). These results suggest that the expression of PV in INs is not dramatically altered by *Dgcr2* knock-down in the L2/3 PNs.

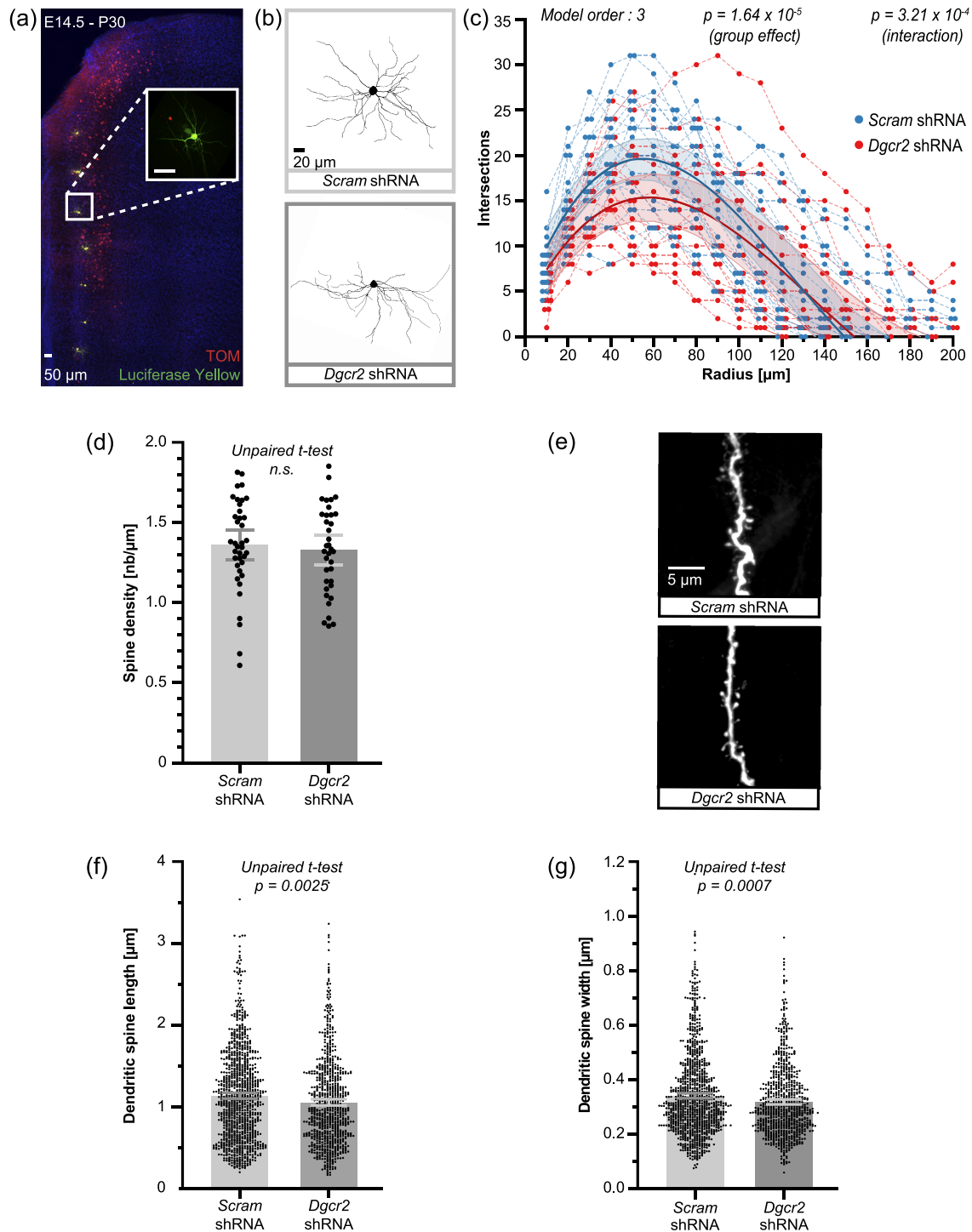


FIGURE 1 *Dgcr2* knock-down alters the complexity of proximal basal dendrites and disrupts the morphological maturation of the second order basal dendritic spines in L2/3 pyramidal neurons of the medial prefrontal cortex at P30. (a) Illustrative image of electroporated PNs in L2/3 of the mPFC that were iontophoretically injected with luciferase yellow; (b) reconstruction of the morphology of the basal dendritic arbor of representative control and *Dgcr2*-knock-down PNs; (c) Scholl analysis of the basal dendritic arbor of control and *Dgcr2*-knock-down PNs. Mixed model regression shows a cubic relationship between the number of intersections and the radius distance. Log-likelihood ratio testing shows a significant ($p < 0.001$) difference between conditions as well as a significant ($p < 0.001$) interaction between condition and radius distance. Using post hoc Bonferroni's multiple comparisons test, only radius 60 reaches statistical significance level ($p = 0.0463$). $n = 15$ – 19 cells, from five mice per condition. (d) *Dgcr2* knock-down does not affect the overall density of dendritic spines ($n = 36$ – 38 cells). Error bars = 95% confidence interval (C.I.). (e) Illustrative image of control and *Dgcr2*-knock-down basal dendritic spines. (f, g) Morphology analysis of the dendritic spines. The length and the width of dendritic spines are reduced by *Dgcr2* knock-down ($n = 801$ – 1043 spines)

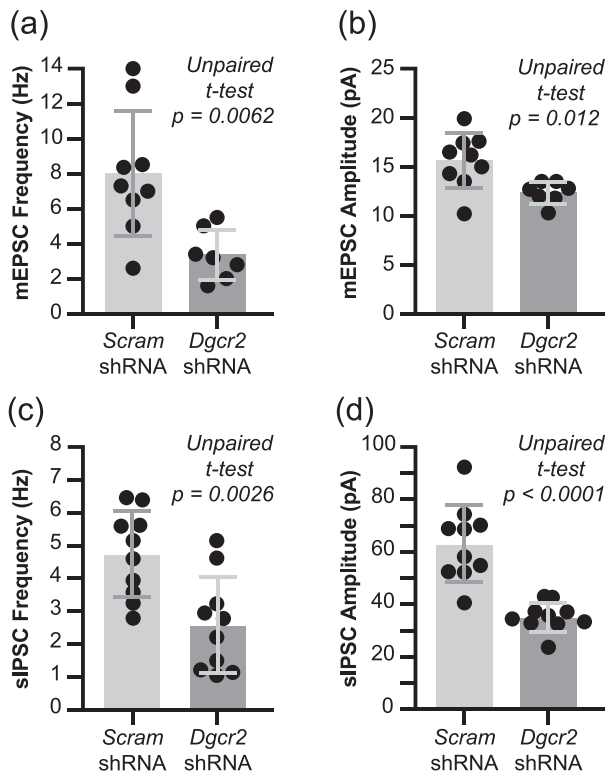


FIGURE 2 *Dgcr2* knock-down reduces the amplitude and the frequency of miniature excitatory post-synaptic currents and spontaneous inhibitory post-synaptic currents of L2/3 pyramidal neurons of the medial prefrontal cortex at P30. (a, b) Miniature (m) EPSCs recorded in layer (L) 2/3 PNs in the mPFC at P30 after E14.5 electroporation are decreased in frequency and amplitude in the *Dgcr2* knock-down condition, demonstrating a functional impact of the dysmaturation profile observed in the dendritic spines maturation of *Dgcr2* knock-down PNs at the same age. $n = 7$ – 9 cells from two mice (*Dgcr2* group) and three mice (*scram* group). (c, d) Spontaneous (s) IPSCs recorded in L2/3 PNs in the mPFC at P30 after E14.5 electroporation are decreased in frequency and amplitude in the *Dgcr2* knock-down condition, suggesting a dysregulation of the connected inhibitory interneurons. $n = 10$ cells, from three mice in each group. Error bars = S.D.

Immunohistochemistry for WFA in our model revealed that the fraction of WFA + PV INs was not different between control and *Dgcr2* knock-down conditions (Figure 3a,e). The perinuclear immunoreactivity for GAD67 around the electroporated PNs, representing a visual proxy for perisomatic inhibitory synapses, was not affected by *Dgcr2* knock-down at P30 in the mPFC regardless of their laminar positioning (Figure 3f–h). Overall, these findings show that the maturation process of PV INs subpopulation in the mPFC is not severely impacted by *Dgcr2* knock-down in PNs at P30.

Altogether, these results demonstrate that *Dgcr2* plays a role in the laminar positioning of upper-layer

PNs in the mPFC at P0.5, proving that this schizophrenia-risk gene acts on neuronal migration across various cortical areas. *Dgcr2* knock-down also impacts the maturation of upper-layer PNs at P30, altering the complexity of proximal basal dendrites and the morphology of the second order basal dendritic spines. More specifically, the reduced width of dendritic spines as well as the reduced proportion of mushroom-type spines that we highlighted are in accordance with previous reports in schizophrenia mice models (Fénelon et al., 2013; Xu et al., 2013).

Additionally, the functional dendritic maturation of *Dgcr2* knock-down PNs is disrupted, as demonstrated by electrophysiological recordings of spontaneous mEPSC at P30. Interestingly, sIPSC are also altered by *Dgcr2* knock-down, but morphological studies of the PV INs in the local microcircuit revealed that the expression of PV and the development of PNN are not dramatically impacted in our model. The perisomatic GAD67 puncta intensity was also unchanged by *Dgcr2* knock-down in PNs, but this result does not completely rule out an involvement of perisomatic inhibition in the changes observed in the inhibitory alterations of *Dgcr2* knock-down PNs, since other synaptic proteins are involved. Further studies of postsynaptic features such as GABA receptors or Gephyrin clusters (Virtanen et al., 2018) could help us correlate our electrophysiological findings with structural alterations in the inhibitory synapses of *Dgcr2* knock-down PNs. Perisomatic inhibition is the main modulator of sIPSC (Miles et al., 1996), but other non-perisomatic inhibitory synapses, such as dendritic synapses, should be explored in order to better understand the microcircuit alteration in our model.

Although we did not directly study the electrophysiological maturation of PV INs—and therefore, we cannot completely rule out their contribution to the observed sIPSC alterations—the preserved postnatal morphological maturation of PV INs in our model suggests that other subtypes of INs (Lim et al., 2018) could participate to the altered sIPSC observed in *Dgcr2* knock-down PNs. An interesting subpopulation for further studies are 5HT3aR INs, because they also participate in corticogenesis deficits linked to vulnerability towards psychiatric disorders (Vitalis et al., 2013) and they regulate the dendritic maturation of PN (Chameau et al., 2009). Future studies should also explore the behavioral correlates of the reported neural alterations in our model. Based on previous studies (Niwa et al., 2010), one could postulate that *Dgcr2* knock-down in the upper-layer PNs of the mPFC could alter schizophrenia-related phenotypes such as prepulse inhibition and/or mPFC-dependent behaviors such as set shifting (Hamilton & Brigman, 2015). Overall, this study reveals a direct effect of *Dgcr2* knock-down on

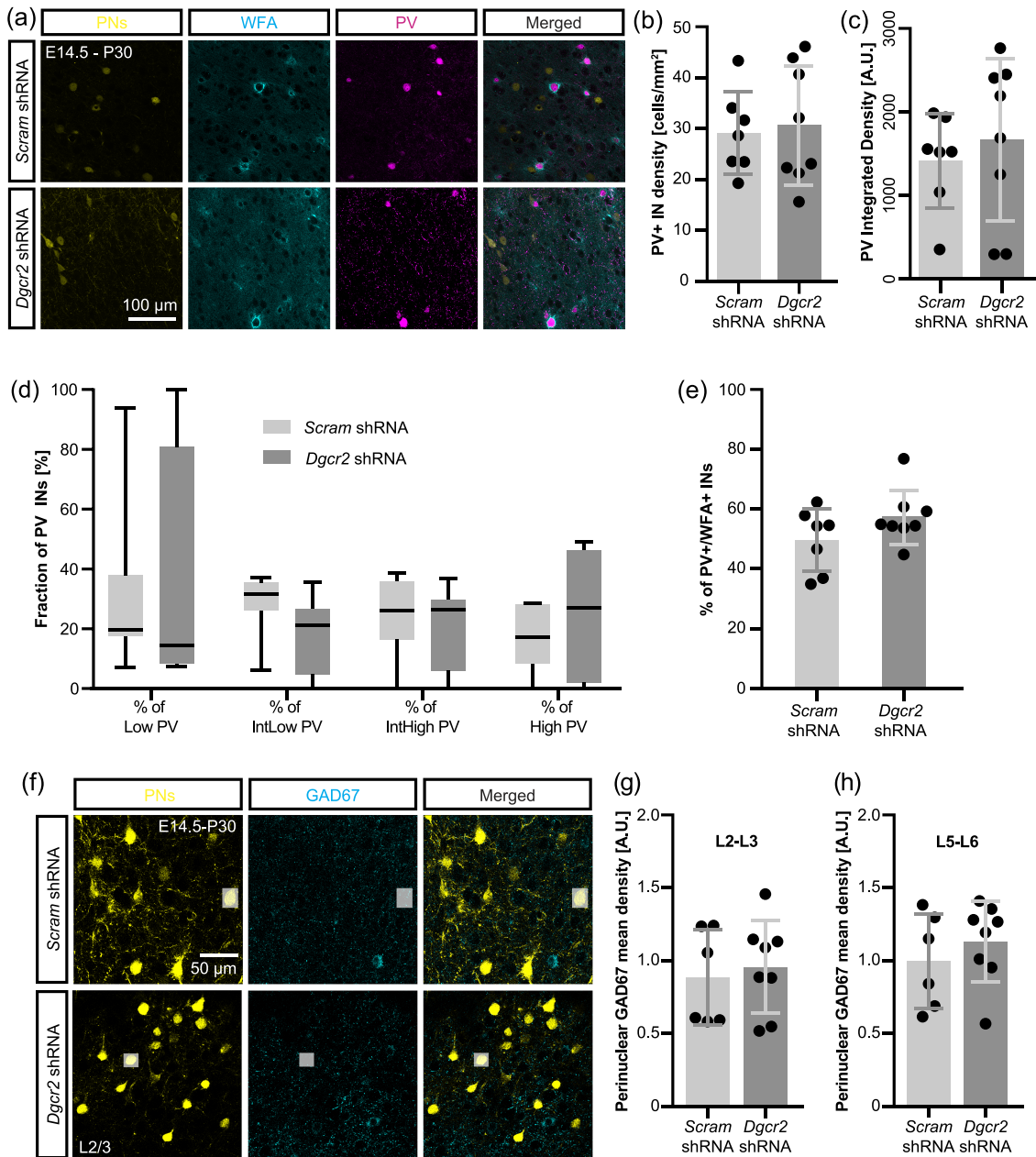


FIGURE 3 *Dgcr2* knock-down in L2-3 pyramidal neurons does not affect the histological development of parvalbumin interneurons in the medial prefrontal cortex at P30. (a) Illustrative images of immunohistochemistry for *Wisteria floribunda* agglutinin (WFA) and parvalbumin (PV) in the mPFC at P30 after E14.5 electroporation of PN with Tomato (TOM) and *Dgcr2* or *Scram* shRNA. (b) The density of PV + INs is not altered by *Dgcr2* knock-down in L2-3 PNs. Error bars = S.D. A.U. = arbitrary unit. (c, d) The PV intensity and the distribution of PV intensities among PV + interneurons (INs) are not altered by *Dgcr2* knock-down in L2-3 PNs. Error bars in c = S.D. (e) The percentage of WFA + PV + INs is not altered by *Dgcr2* knock-down in L2-3 PNs. Error bars = S.D. (f) Representative images of IHC for GAD67, white circles around PNs display an illustrative region of interest (ROI) used for the following analysis. (g, h) The mean density of GAD67 IHC in perinuclear region of E14.5 electroporated PNs is not changed by *Dgcr2* knock-down in L2-3 PNs, regardless of their laminar positioning. Error bars = S.D. $n = 6-8$ mice, from three different litters

the functional maturation of PNs in the mPFC and highlights an intriguing non-cell-autonomous effect of *Dgcr2* knock-down in upper-layer PNs on the maturation of the mPFC microcircuit, opening the way to further experiments that could unfold the diversity of the cell lineages at play in schizophrenia.

ACKNOWLEDGMENTS

The authors wish to thank the Bioimaging Core Facility of the Faculty of Medicine of Geneva for assistance in the image acquisition.

This work was supported by the Institute of Genetics and Genomics of Geneva (to AMC and AD), the Vachoux

Foundation (to AMC) and by the NCCR Synapsy (51NF40-185897) (to AD). Open Access Funding provided by Universite de Geneve.

CONFLICT OF INTEREST

The authors declare that the research was conducted in the absence of any commercial or financial relationships that could be construed as a potential conflict of interest.

AUTHOR CONTRIBUTIONS

AMC and AD designed the experiments. AMC wrote the original draft; all other authors (except AD) critically reviewed the article. AMC performed in utero electroporations, laminar positioning, dendritic spine density and all immunohistochemistry studies. MG performed the dendritic spine morphological study and the statistical analysis of the dendritic arbor study. AR performed the dendritic arbor image analysis. TB performed the iontophoretic injection, supervised by LV. CB performed the mEPSC study and SM did the sIPSC study. All authors except AD approved the final manuscript.

DATA AVAILABILITY STATEMENT

The data that support the findings of this study are available from the corresponding author upon reasonable request.

ORCID

Aude Molinard-Chenu  <https://orcid.org/0000-0002-2552-9520>

REFERENCES

- Beasley, T. M., & Schumacker, R. E. (1995). Multiple regression approach to analyzing contingency tables: Post hoc and planned comparison procedures. *The Journal of Experimental Education, 64*, 79–93. <https://doi.org/10.1080/00220973.1995.9943797>
- Berretta, S., Pantazopoulos, H., Markota, M., Brown, C., & Batzianouli, E. T. (2015). Losing the sugar coating: Potential impact of perineuronal net abnormalities on interneurons in schizophrenia. *Schizophrenia Research, 167*, 18–27. <https://doi.org/10.1016/j.schres.2014.12.040>
- Cabungcal, J.-H., Counotte, D., Lewis, E., Tejada, H., Piantadosi, P., Pollock, C., Calhoun, G., Sullivan, E., Presgraves, E., Kil, J., Hong, L. E., Cuenod, M., Do, K. Q., & O'Donnell, P. (2014). Juvenile antioxidant treatment prevents adult deficits in a developmental model of schizophrenia. *Neuron, 83*(5), 1073–1084. <https://doi.org/10.1016/j.neuron.2014.07.028>
- Chameau, P., Inta, D., Vitalis, T., Monyer, H., Wadman, W. J., & van Hooft, J. A. (2009). The N-terminal region of reelin regulates postnatal dendritic maturation of cortical pyramidal neurons. *Proceedings of the National Academy of Sciences, 106*, 7227–7232. <https://doi.org/10.1073/pnas.0810764106>
- Crabtree, G. W., & Gogos, J. A. (2014). Synaptic plasticity, neural circuits, and the emerging role of altered short-term information processing in schizophrenia. *Front. Synaptic Neurosci., 6*, 28. <https://doi.org/10.3389/fnsyn.2014.00028>
- Curley, A. A., Arion, D., Volk, D. W., Asafu-Adjiei, J. K., Sampson, A. R., Fish, K. N., & Lewis, D. A. (2011). Cortical deficits of glutamic acid decarboxylase 67 expression in schizophrenia: Clinical, protein, and cell type-specific features. *Am J Psychiat, 168*(9), 921–929. <https://doi.org/10.1176/appi.ajp.2011.11010052>
- de Roo, M., & Ribic, A. (2017). Analyzing structural plasticity of dendritic spines in organotypic slice culture. In *Methods in molecular biology* (pp. 277–289). Humana Press Inc.. https://doi.org/10.1007/978-1-4939-6688-2_19
- Enwright, J., Sanapala, S., Foglio, A., Berry, R., Fish, K., & Lewis, D. (2016). Reduced labeling of parvalbumin neurons and perineuronal nets in the dorsolateral prefrontal cortex of subjects with schizophrenia. *Neuropsychopharmacology, 41*(9), 2206–2214. <https://doi.org/10.1038/npp.2016.24>
- Fénelon, K., Xu, B., Lai, C. S., Mukai, J., Markx, S., Stark, K. L., Hsu, P. K., Gan, W. B., Fischbach, G. D., MacDermott, A., Karayiorgou, M., & Gogos, J. A. (2013). The pattern of cortical dysfunction in a mouse model of a schizophrenia-related microdeletion. *The Journal of Neuroscience, 33*(37), 14825–14839. <https://doi.org/10.1523/JNEUROSCI.1611-13.2013>
- Ferguson, B. R., & Gao, W. J. (2018). PV interneurons: Critical regulators of E/I balance for prefrontal cortex-dependent behavior and psychiatric disorders. *Front. Neural Circuits, 12*, 37. <https://doi.org/10.3389/fncir.2018.00037>
- Freund, T. F., & Katona, I. (2007). Perisomatic inhibition. *Neuron, 56*, 33–42. <https://doi.org/10.1016/j.neuron.2007.09.012>
- Glausier, J. R., & Lewis, D. A. (2013). Dendritic spine pathology in schizophrenia. *Neuroscience, 251*, 90–107. <https://doi.org/10.1016/j.neuroscience.2012.04.044>
- Glausier, J. R., & Lewis, D. A. (2018). Mapping pathologic circuitry in schizophrenia. In *Handbook of clinical neurology* (Vol. 150) (pp. 389–417). Elsevier B.V. <https://doi.org/10.1016/B978-0-444-63639-3.00025-6>
- Hamilton, D. A., & Brigman, J. L. (2015). Behavioral flexibility in rats and mice: Contributions of distinct frontocortical regions. *Genes, Brain Behav., 14*, 4–21. <https://doi.org/10.1111/gbb.12191>
- Haws, M. E., Jaramillo, T. C., Espinosa, F., Widman, A. J., Stuber, G. D., Sparta, D. R., Tye, K. M., Russo, S. J., Parada, L. F., Stavarache, M., Kaplitt, M., Bonci, A., & Powell, C. M. (2014). PTEN knockdown alters dendritic spine/protrusion morphology, not density. *The Journal of Comparative Neurology, 522*(5), 1171–1190. <https://doi.org/10.1002/cne.23488>
- Lewis, D. A. (2014). Inhibitory neurons in human cortical circuits: Substrate for cognitive dysfunction in schizophrenia. *Current Opinion in Neurobiology, 26*, 22–26. <https://doi.org/10.1016/j.conb.2013.11.003>
- Lewis, D. A., Hashimoto, T., & Volk, D. W. (2005). Cortical inhibitory neurons and schizophrenia. *Nature Reviews. Neuroscience, 6*, 312–324. <https://doi.org/10.1038/nrn1648>
- Lim, L., Mi, D., Llorca, A., & Marin, O. (2018). Development and functional diversification of cortical interneurons. *Neuron, 100*, 294–313. <https://doi.org/10.1016/j.neuron.2018.10.009>
- Mancini, V., Sandini, C., Padula, M. C., Zöllner, D., Schneider, M., Schaefer, M., & Eliez, S. (2020). Positive psychotic symptoms are

- associated with divergent developmental trajectories of hippocampal volume during late adolescence in patients with 22q11DS. *Molecular Psychiatry*, 25, 2844–2859. <https://doi.org/10.1038/s41380-019-0443-z>
- Miles, R., Tóth, K., Gulyás, A. I., Hájos, N., & Freund, T. F. (1996). Differences between somatic and dendritic inhibition in the hippocampus. *Neuron*, 16, 815–823. [https://doi.org/10.1016/S0896-6273\(00\)80101-4](https://doi.org/10.1016/S0896-6273(00)80101-4)
- Molinard-Chenu, A., & Dayer, A. (2018). The candidate schizophrenia risk gene DGCR2 regulates early steps of corticogenesis. *Biological Psychiatry*, 83, 692–706. <https://doi.org/10.1016/j.biopsych.2017.11.015>
- Muraki, K., & Tanigaki, K. (2015). Neuronal migration abnormalities and its possible implications for schizophrenia. *Frontiers in neuroscience*, 9, 74. <https://doi.org/10.3389/fnins.2015.00074>
- Mutlu, A. K., Schneider, M., Debbané, M., Badoud, D., Eliez, S., & Schaer, M. (2013). Sex differences in thickness, and folding developments throughout the cortex. *NeuroImage*, 82, 200–207. <https://doi.org/10.1016/j.neuroimage.2013.05.076>
- Niwa, M., Kamiya, A., Murai, R., Kubo, K., Gruber, A., Tomita, K., Lu, L., Tomisato, S., Jaaro-Peled, H., Seshadri, S., Hiyama, H., Huang, B., Kohda, K., Noda, Y., O'Donnell, P., Nakajima, K., Sawa, A., & Nabeshima, T. (2010). Knockdown of DISC1 by in utero gene transfer disturbs postnatal dopaminergic maturation in the frontal cortex and leads to adult behavioral deficits. *Neuron*, 65(4), 480–489. <https://doi.org/10.1016/j.neuron.2010.01.019>
- Schubert, D., Martens, G. J. M., & Kolk, S. M. (2015). Molecular underpinnings of prefrontal cortex development in rodents provide insights into the etiology of neurodevelopmental disorders. *Molecular Psychiatry*, 20, 795–809. <https://doi.org/10.1038/mp.2014.147>
- Steullet, P., Cabungcal, J.-H., Coyle, J., Didriksen, M., Gill, K., Grace, A., Hensch, T., LaMantia, A.-S., Lindemann, L., Maynard, T., Meyer, U., Morishita, H., O'Donnell, P., Puhl, M., Cuenod, M., & Do, K. Q. (2017). Oxidative stress-driven parvalbumin interneuron impairment as a common mechanism in models of schizophrenia. *Molecular Psychiatry*, 22(7), 936–943. <https://doi.org/10.1038/mp.2017.47>
- Virtanen, M. A., Laco, C., Fiumelli, H., Kosel, M., Tyagarajan, S., de Roo, M., & Vutskits, L. (2018). Development of inhibitory synaptic inputs on layer 2/3 pyramidal neurons in the rat medial prefrontal cortex. *Brain Structure & Function*, 223, 1999–2012. <https://doi.org/10.1007/s00429-017-1602-0>
- Vitalis, T., Ansoorge, M. S., & Dayer, A. G. (2013). Serotonin homeostasis and serotonin receptors as actors of cortical construction: Special attention to the 5-HT3A and 5-HT6 receptor subtypes. *Frontiers in Cellular Neuroscience*, 7, 93. <https://doi.org/10.3389/fncel.2013.00093>
- Xu, B., Hsu, P.-K., Stark, K. L., Karayiorgou, M., & Gogos, J. A. (2013). Derepression of a novel neuronal inhibitor is a major outcome of miRNA dysregulation due to 22q11.2 microdeletion. *Cell*, 152, 262.

SUPPORTING INFORMATION

Additional supporting information may be found in the online version of the article at the publisher's website.

How to cite this article: Molinard-Chenu, A., Godel, M., Rey, A., Musardo, S., Bodogan, T., Vutskits, L., Bellone, C., & Dayer, A. (2022). Downregulation of the schizophrenia risk-gene *Dgcr2* alters early microcircuit development in the mouse medial prefrontal cortex. *International Journal of Developmental Neuroscience*, 82(3), 277–285. <https://doi.org/10.1002/jdn.10175>